Colloid Polym Sci (2004) 283: 74–83
DOI 10.1007/s00396-004-1094-3

ORIGINAL CONTRIBUTION

Dulce Paloma del J. Gutiérrez-Hijar
Fausto Becerra
J. E. Puig
J. Félix Armando Soltero-Martínez
María Belén Sierra
Pablo C. Schulz

Properties of two polymerizable surfactants aqueous solutions: dodecylethylmethacrylatedimethylammonium bromide and hexadecylethylmethacrylatedimethylammonium bromide. I. Critical micelle concentration

Received: 5 December 2003
Accepted: 3 March 2004
Published online: 19 June 2004

D. P. del J. Gutiérrez-Hijar · F. Becerra
J. E. Puig · J. F. A. Soltero-Martínez
Departamento de Ingeniería Química,
CUCEI, Universidad de Guadalajara,
44430 Guadalajara, Jalisco, México

M. B. Sierra · P. C. Schulz (✉)
Departamento de Química, Universidad
Nacional del Sur, 8000 Bahía Blanca,
Buenos Aires, Argentina
E-mail: pschulz@criba.edu.ar

Abstract The aggregation of two polymerisable surfactants dodecylethylmethacrylatedimethylammonium bromide (C_{12}PS) and hexadecylethylmethacrylatedimethylammonium bromide (C_{16}PS) was studied with a battery of methods. Both surfactants form premicelles at low concentration, and show a critical micelle concentration and a transition between spherical and rod-like micelles. The micelle ionization degree and the adsorption at the air/solution interface were also studied. Results are interpreted on the basis of the conformation of the polar head group.

Keywords Alkylethylmethacrylatedimethylammonium bromides · Critical micelle concentration · Polymerizable surfactants · Adsorption · Micelle ionization degree

Introduction

Surfactant molecules with chemically active groups have received increased attention in recent years. Since these materials can often be polymerized or oligomerized, a wide range of uses can be foreseen. Polymerizable surfactants can be polymerized to yield polysoaps, which can form hydrophobic microdomains having properties similar to surfactant micelles [1, 2]. They may also be copolymerized with water-soluble or water-insoluble monomers [3, 4, 5]. The polymerized structures may be micelles [6, 7], vesicles [8, 9, 10], monolayers [11, 12], bilayers [13, 14], liquid crystals [15, 16], and microemulsions [17, 18, 19].

Knowledge of the phase behavior of polymerizable surfactants is of fundamental importance to the design of the polymerization experiments. Several studies have been made on this subject [20, 21, 22, 23].

Polymerizable amphiphilic compounds carry a vinyl double bound together with hydrophilic and hydrophobic moieties in a molecule. The active double bound may be situated either at the hydrophobic chain or at the hydrophilic headgroup, which may be cationic, anionic or non-ionic.

Polymerizable Surfactants studied in this work, dodecylethylmethacrylatedimethylammonium bromide (C_{12}PS) (= C-12 polymerizable surfactant) and hexadecylethylmethacrylatedimethylammonium bromide (C_{16}PS) have the following polar group structure (active site):

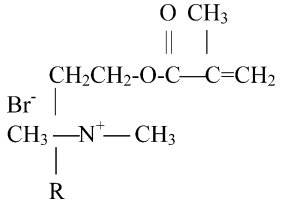

where R is a dodecyl (C_{12}) or hexadecyl radical. There are very few references regarding these surfactants. In 1992 Nika et al. [24] reported the synthesis procedure of C_{12}PS and determined its critical micelle concentration (CMC) using the conductivity method. He also

studied, both the polymerization of the pure monomer and a micellar solution by means of γ radiation.

McGrath and Drummond [25] published the phase diagram of this surfactant, and polymerized it a in liquid crystalline phase. There are some inconsistencies regarding the data of these surfactants. For example, McGrath and Drummond report a CMC = 7.29×10^{-3} mol dm^{-3} [25] for the C_{12}PS, while Nagai et al. [7] found it to be of 6×10^{-3} mol dm^{-3}. Nevertheless Hamid and Sherrington [26] found the CMC value to be of and between 1.9×10^{-3} and 3.6×10^{-3} mol dm^{-3}, depending on the determination method used. The aggregation number of the same non-polymerized surfactant was reported to be 11 [24], and 51 [25]. C_{16}PS data are much more scarce and will be cited within the text.

Experimental

Both surfactants were synthesized using the method described by Nika et al. [24].

Samples were prepared in 40-cm^{3}vials, in concentration ranging from 10^{-4} to 10^{-3} wt% for the dodecylethylmethacrylatedimethylammonium bromide (C_{12}PS) and from 10^{-3} to 10^{-2} wt% for the hexadecylethylmethacrylatedimethylammonium bromide (C_{16}PS). Vials were subsequently sealed and manually stirred. They were then left ten days in a thermostat bath at 25 °C and were periodically and gently stirred.

Conductivity measurements were made with an Orion Mod 122 conductimeter and an immersion cell having four graphite electrodes. The device was calibrated with a KCl solution. Measurements were performed twice by titration of 50 mL water with each concentration solution. Shaking and the subsequent conductivity determination followed each addition of 0.5 mL of concentrated surfactant mixture solution.

Surface tension measurements were made with a K 10ST Krüss tensiometer and Wilhelmy plate. Each measurement was performed twice to obtain coherent values, allowing a rest time of almost 15 min between the sample addition and the surface tension measurement to allow for the surface adsorption to be achieved.

Sudan III solubilization experiments were made by adding a small quantity of solid dye to vials having surfactant solutions. Then vials were hermetically closed and left in a thermostatic bath for four days to allow for solubilization equilibrium to be achieved. Vials were shaken each day. After centrifugation, the supernatant absorbance was measured with a Perkin-Elmer Lambda 11B spectrophotometer at 600 nm.

Viscosity measurements were made with a Fenske-Cannon 50 Q977 Ostwald viscosimeter calibrated with water.

The density measurements were performed with a pycnometer.

The Student t function was employed to compute the error intervals. Confidence level was 0.90.

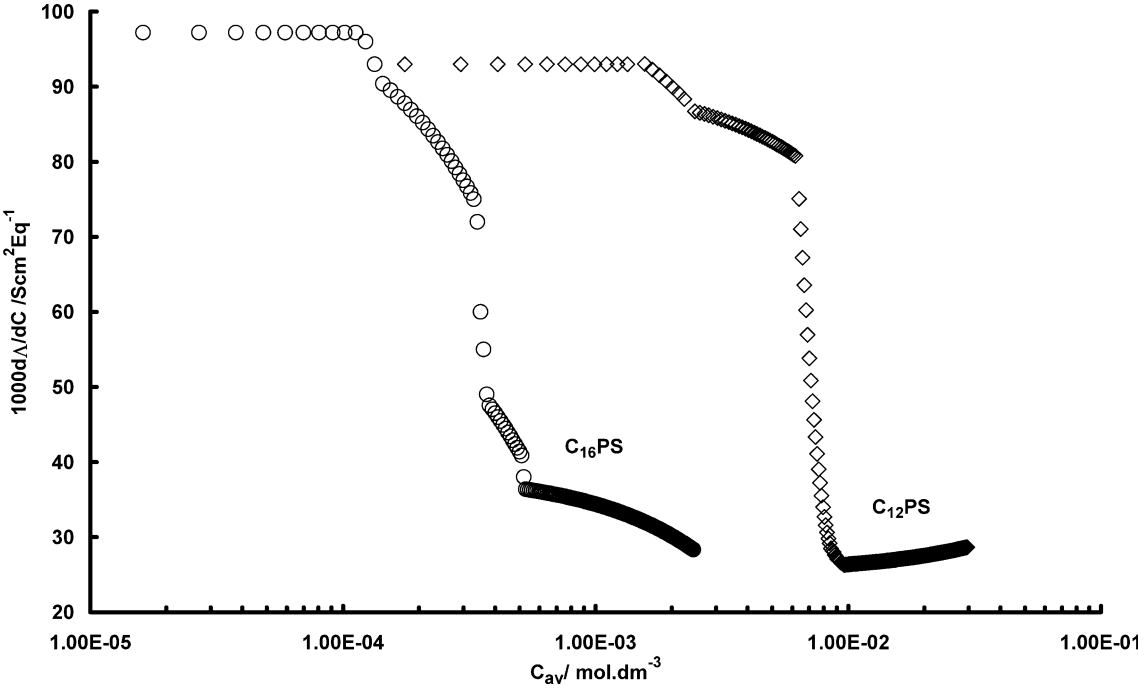

Fig. 1 Differential conductivity of C_{12}PS (*open diamonds*) and C_{16}PS (*open circles*) aqueous solutions as a function of the average concentration

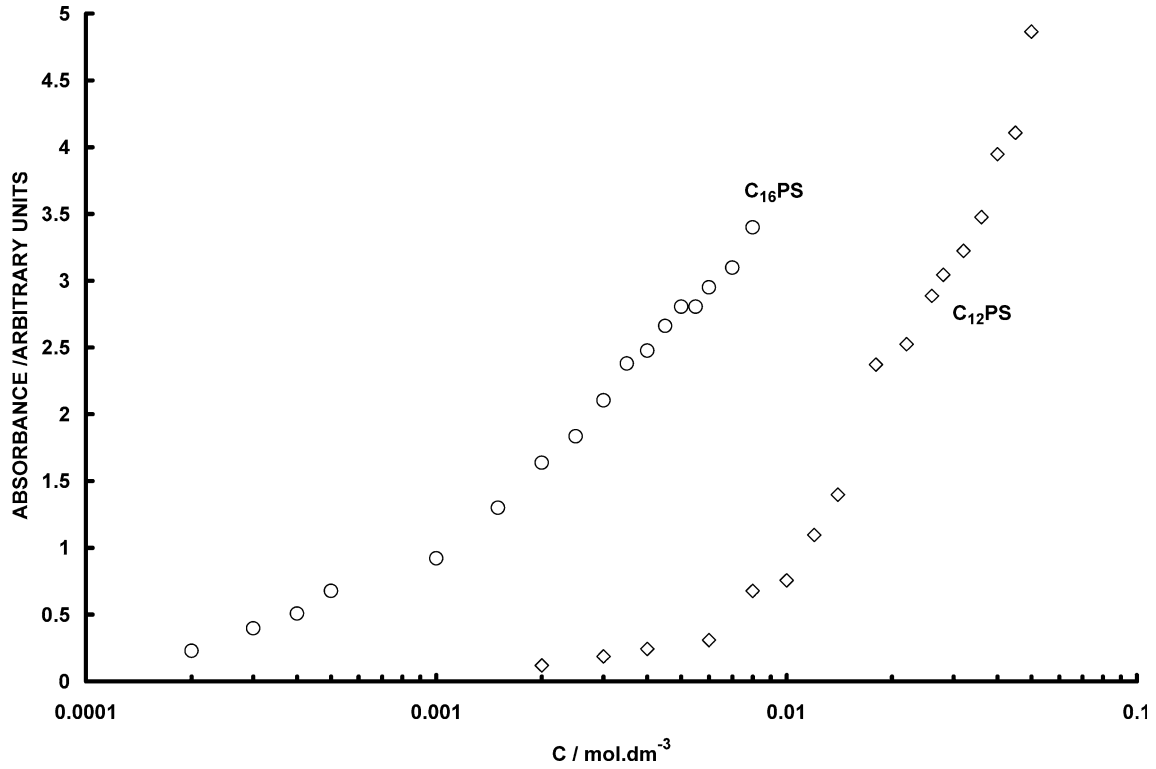

Fig. 2 Sudan III solubilization by $C_{12}PS$ (*open diamonds*) and $C_{16}PS$ (*open circles*) aqueous solutions vs surfactant concentration

Results

Figure 1 shows the differential conductivity $1000d\kappa/dC$ vs as a function of the medium concentration C_{av} of both surfactants, computed from the specific conductivity.

Figure 2 shows the Sudan III solubilization absorbance of both surfactants solutions. The extrapolation to zero absorbance gives $C = 9.9\times10^{-6}$ mol dm^{-3} for $C_{12}PS$ and $C = 4.1\times10^{-6}$ mol dm^{-3} for $C_{16}PS$.

Figure 3 shows the density dependence of both surfactants solutions on the concentration.

Figure 4 illustrates the dependence of surface tension on the logarithm of the concentration for both surfactants.

Figure 5 shows the viscosity as a function of the concentration for both surfactants.

Figure 6 shows absorbance of both surfactant solutions as a function of the concentration at 253.3 nm ($C_{12}PS$), and 274 nm ($C_{16}PS$), the wavelength at which the surfactant's spectrum has a maximum.

Discussion

To allow for the best study of the conductivity of the surfactants, the specific conductivity vs concentration curves of both surfactants were fitted. The objective was to minimize the effect of minimum deviations on the calculation of differential conductivity.

$C_{12}PS$

The differential conductivity $1000d\kappa/dC$ of $C_{12}PS$ (Fig. 1) shows two steps, indicating structural changes, the first related to the CMC, and the second to the formation of elongated micelles. The representation of $\Delta\kappa = \kappa - \kappa_{extrapol}$ as a function of the total concentrations for the $C_{12}PS$ (not shown), where $\kappa_{extrapol}$ is the extrapolated specific conductivity from the specific conductivity below the CMC value, also show two breaks in the dependency of the conductivity with the concentration.

Table 1 shows the concentrations at which the transitions of the dependency of the different properties on the $C_{12}PS$ concentration were found. A total of three concentrations at which such transitions occurred were observed; $C_1 = (7.78 \pm 0.27)\times10^{-4}$ mol dm^{-3}, $C_2 = (1.88 \pm 0.31)\times10^{-3}$ mol dm^{-3}, and $C_3 = (6.94 \pm 0.36)\times10^{-3}$ mol dm^{-3}.

Figure 1 shows that there are two transitions affecting the number of conductive species in solution and their conductive capacity, these processes being generally related to the formation of micelles and micellar structure changes. These transitions occurred at C_2 and C_3. However, Fig. 2 shows that there is Sudan III solubilization even below C_2, which could be an indication

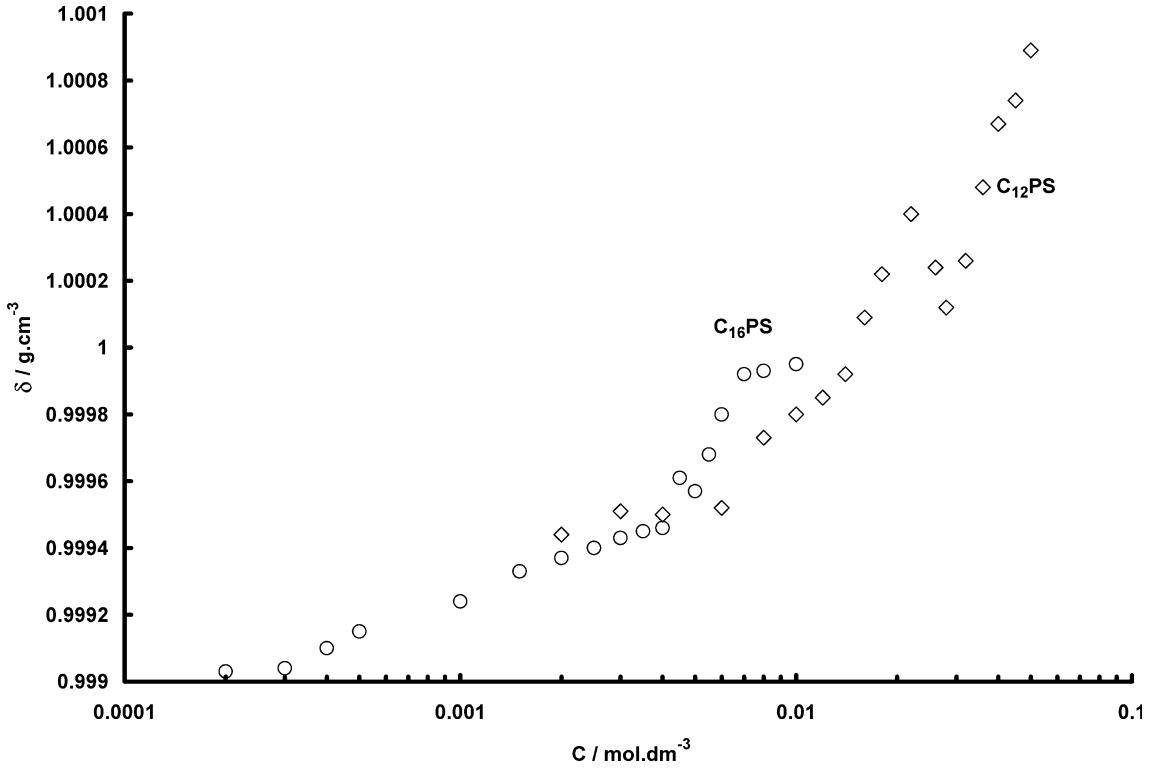

Fig. 3 Dependence of the density of $C_{12}PS$ (*open diamonds*) and $C_{16}PS$ (*open circles*) aqueous solutions on the surfactant concentration

of the presence of dimers or premicelles with solubilising capacity.

Surfactant solutions that form premicellar aggregates may solubilize water-insoluble substances below the CMC [27, 28, 29]. Figure 3 also shows modifications in the density vs C dependence, which might be an indication of structural changes. The dependency of the surface tension the logarithm of the concentration (Fig. 4) reveals two changes, again at C_2 and C_3, and the dependency of the viscosity with the concentration (Fig. 5) identifies the transition in C_3 as a change of an isomeric structure (spherical) towards an anisometric one (cylindrical).

Consequently, C_2 can be identified as the critical micellar concentration, where the micelles are formed. A glance on Fig. 1 indicates that the structure of the spherical micelles formed must be dependent on the concentration, due to the curvature between C_2 and C_3in the $\Delta\kappa$ vs C graph (not shown), and the high value of the slope in the same region, in Fig. 1. The absence of linearity in Fig. 3 suggests the same conclusion. A representation of the absorbance/concentration ratio as a function of the concentration (Fig. 7) shows that after the CMC there is an increment of the solubilising capacity with increasing concentration, also indicating that the structure of the aggregates is changing and that these are becoming more and more efficient in the solubilization of the dye in the hydrocarbon core. This situation arises frequently in solutions of surfactants where micelles have a low aggregation number at the CMC, and where the size and structure of these micelles suffer a significant change with the total concentration, as was found in some sodium alkanephosphonates [30, 31, 32, 33, 34]. Above C_3, the solubilising capacity decreases quickly, which is in accordance with an increase in length of cylindrical micelles, provided that the solubilising capacity does not increase in the same proportion as the chain length. Figure 4 indicates that spherical micelles are not much more energetically favorable than the adsorption of monomers in the air/solution interface; thus surface tension will continue to decrease. The size of the unpolymerized $C_{12}PS$ micelles is $n_{C12PS} = 11$ [24]. Such small micelles must have a great proportion of the hydrocarbon chains in contact with water, increasing the free energy per molecule. In contrast, some 10% to 30% of the hydrocarbon chain length of the molecules adsorbed at the air/solution interface are in contact with water [35, 36, 37, 38]. Only the cylindrical micelles are energetically favorable enough to reduce the adsorption in the air/solution interface, due to the compactness of the hydrocarbon core and the reduction in the area per polar group at the surface of the micellar structure.

For comparison, the CMC of allyldimethyldodecylammonium bromide is 1.25×10^{-2} mol dm^{-3} [39] or 1.20×10^{-2} mol dm^{-3} [40].The CMC of dodecyltrime-

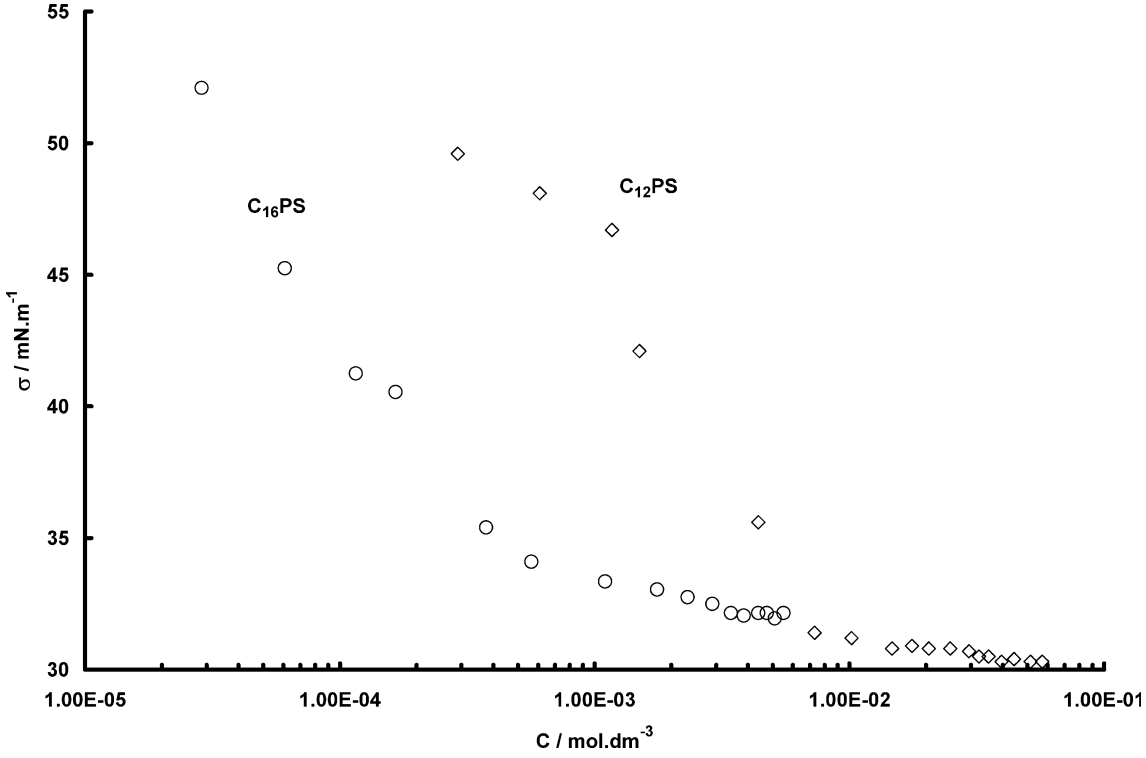

Fig. 4 Surface tension of $C_{12}PS$ (*open diamonds*) and $C_{16}PS$ (*open circles*) aqueous solutions as a function of the logarithm of surfactant concentration

thylammonium bromide (DTAB) is 1.44×10^{-2} mol dm^{-3} [41].

McGrath and Drummond found that the $C_{12}PS$ CMC was 7.29×10^{-3} mol dm^{-3} [25] Nagai et al. [7] found CMC $= 6\times10^{-3}$ mol dm^{-3}, but Hamid and Sher-

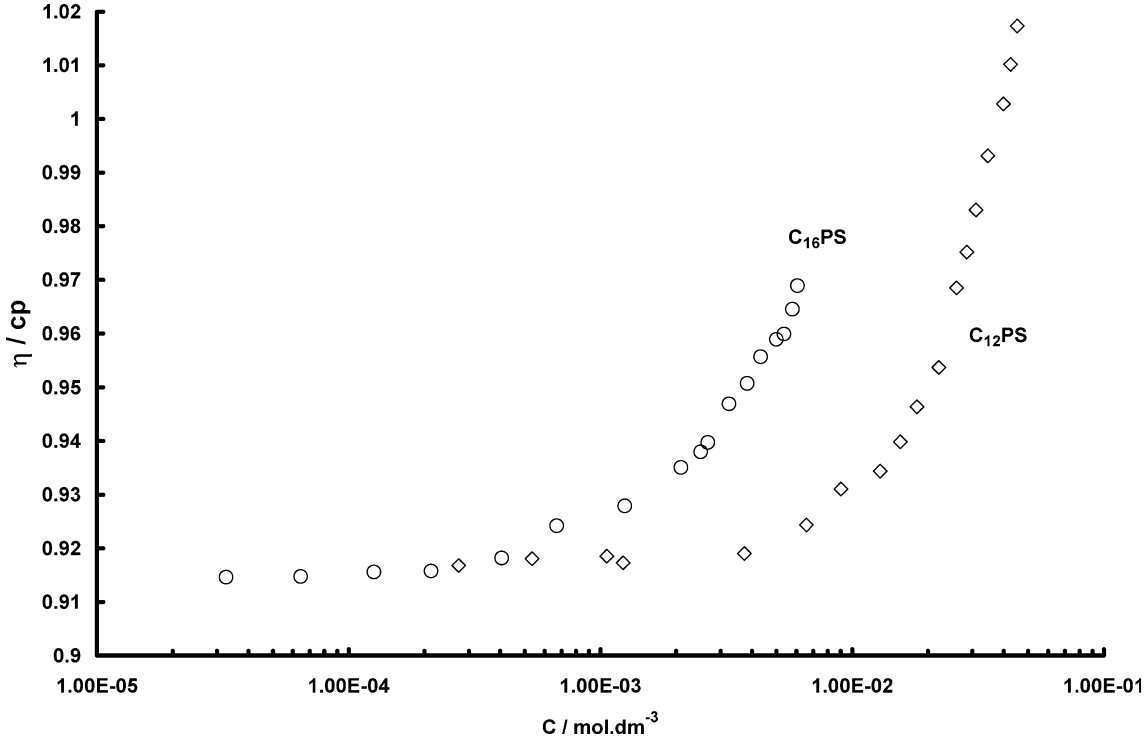

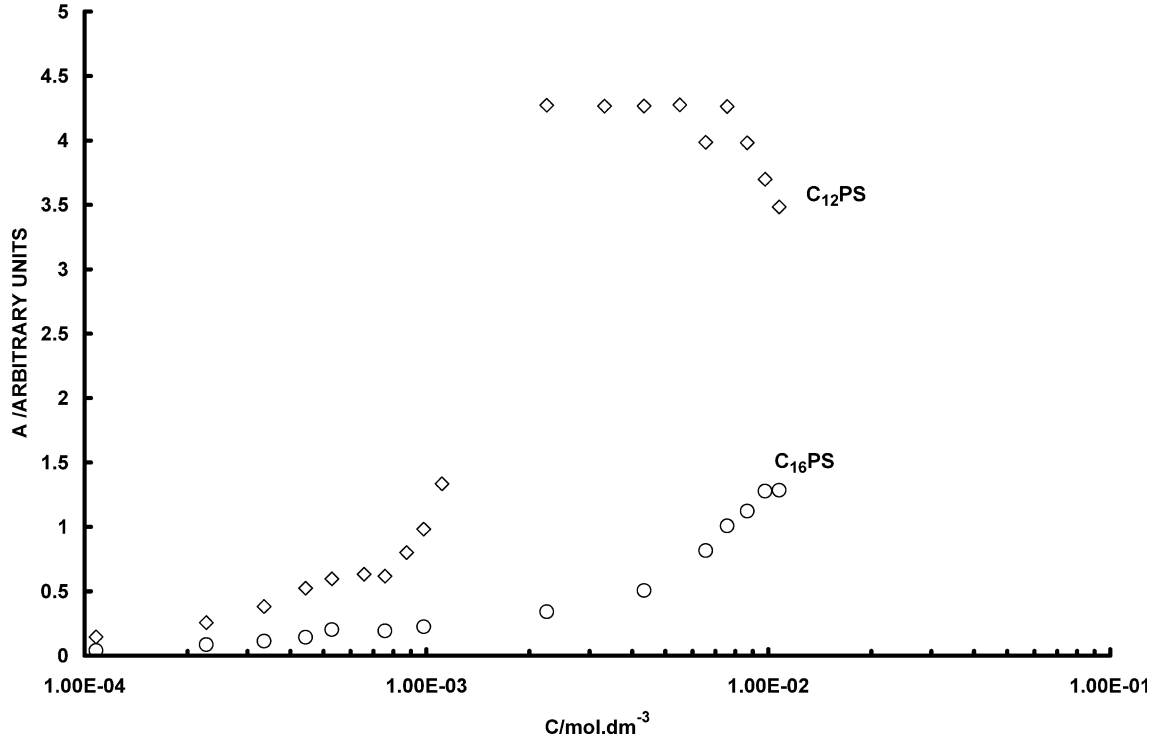

Fig. 6 Absorbance of $C_{12}PS$ (*open diamonds*) (at $\lambda = 253.3$ nm) and $C_{16}PS$ (*open circles*) (at $\lambda = 274$ nm) aqueous solutions without added dye, as a function of the surfactant concentration

rington [26] found that the CMC was between 1.9×10^{-3} and 3.6×10^{-3} mol dm^{-3}, depending on the method employed in its determination. Based on the above results, it is evident that McGrath and Drummond, and Nagai et al. have confounded the transition spherical micelles↔rod-like micelles (C_3) with the CMC (C_2). This may be caused by the small size of micelles at C_2, that renders its detection difficult by conductivity and surface tension measurements.

Hamid and Sherrington [26] proposed an annular structure of the polar head group with six links (three carbon, one nitrogen, and two oxygen atoms) via intramolecular interaction between the carbonyl oxygen of the methylmethacrylate radical and the positively charged nitrogen:

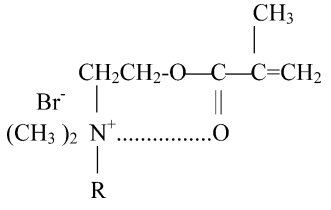

◄

Fig. 5 Viscosity of $C_{12}PS$ (*open diamonds*) and $C_{16}PS$ (*open circles*) aqueous solutions vs surfactant concentration

The zwitterionic surfactant dodecyldimethyl 4-propionate ammonium (DDPA: $CH_3(CH_2)_{11}N^+(CH_3)_2$-$(CH_2)_3COO^-$) may have the same conformation of polar headgroup. Its CMC is 0.0043 mol dm^{-3}, and that of dodecyldimethyl 6-hexanoate ammonium (DDHA, $CH_3(CH_2)_{11}N^+(CH_3)_2$-$(CH_2)_5COO^-$) 0.0026 mol dm^{-3} [42]. In comparison, the CMC of hexadecyltrimethylammonium bromide (HTAB) is 0.0013 mol dm^{-3} [43]. This suggests that the short hydrocarbon chain in the polar head group probably increases the total hydrophobicity of the molecule, as suggested by Hamid and Sherrington with respect to the C_nPS surfactants [26]. However, the suggestion of these authors of simply adding the extra methylene groups to the hydrocarbon chain seems excessively simple. When the CMCs of $C_{12}PS$ ($(1.88\pm0.31)\times10^{-3}$ mol dm^{-3}) and tetradecyltrimethylammonium bromide (TTAB, CMC = 3.41×10^{-3} mol dm^{-3}) [44], and that of HTAB (0.0013 mol dm^{-3}) and DDPA (0.0043 mol dm^{-3}), are compared, it may be seen that the situation is more complex. The change in hydrophilicity of the polar head group must also be taken into account. This change is related to both, the change in counterion, and the effective charge of the polar group. As an example, the CMC of hexadecyltrimethylammonium chloride (HTAC) is 0.0009 mol dm^{-3} [45, 46], about 13% lower than that of HTAB, caused by the change in counterion. A one e unit reduction in the charge of the polar head group reduces the CMC by about one order of magnitude [47]. In both surfactant pairs ($C_{12}PS$-TTAB and DDPA-HTAB) there

Table 1 Transitions observed in $C_{12}PS$ solutions, in mol·dm^{-3}

Method	C_1	C_2	C_3
Λ(log C)	0.000816	0.00173	0.00685
$\Lambda(\sqrt{C})$	0.000818	0.00173	0.00676
$1000d\kappa/dC(C_{av})$	-	0.00202	0.007
$\Delta\kappa$(C)	-	0.0023	0.00665
κ(C)	-	0.00196	0.0073
σ(log C)	-	0.00117	0.00737
δ(C)	-	-	-
A(C)	0.000756	0.00225	0.00758
η(C)	-	-	0.006
Sudan III	0.0008	-	-
Average value	$(7.78 \pm 0.27)\times10^{-4}$	$(2.02 \pm 0.53)\times10^{-3}$	$(6.94 \pm 0.36)\times10^{-3}$

is a discrepancy between the expected CMC obtained by simply adding the extra methylene groups to the hydrocarbon chain of the alkyltrimethylammonium halide and the experimental one. In the DDPA-HTAB pair, this difference may be interpreted by an increase in the polarity of the $N^+(CH_3)_2$-$(CH_2)_3COO^-$group with respect to the $N^+(CH_3)_3$one, because of the charge carried by the carboxylate group. This causes a CMC about 23% higher than that expected. In the $C_{12}PS$-TTAB pair, if the ring suggested by Hamid and Sherrington is formed, there is a loss of polarity of the group $N^+(CH_3)_2...O=C$-O-R when compared with the $N^+(CH_3)_3$one, because of a charge delocalization. This causes a reduction of the CMC of about 45%. The weak polarity of the oxygen atoms and the hydrophilicity of the double bond would not be enough to compensate the effect of this delocalization.

The annular conformation proposed by Hamid and Sherrington may also explain the yellowish color of both surfactant solutions ($C_{12}PS$ and $C_{16}PS$), This color is produced by the excitation of the delocalized electrons. In that case, a change in the conformation of the ring may occur because of the crowding produced when micelles form, and when the structure of micelles changes. As an example, a large change of reduction in the area per micellized head group occurs when spherical micelles become worm-like [48, 49]. These conformational changes must change the absorptivity, and in consequence, the slope of the absorbance-concentration curve must change at the CMC and at the sphere-to-rod-

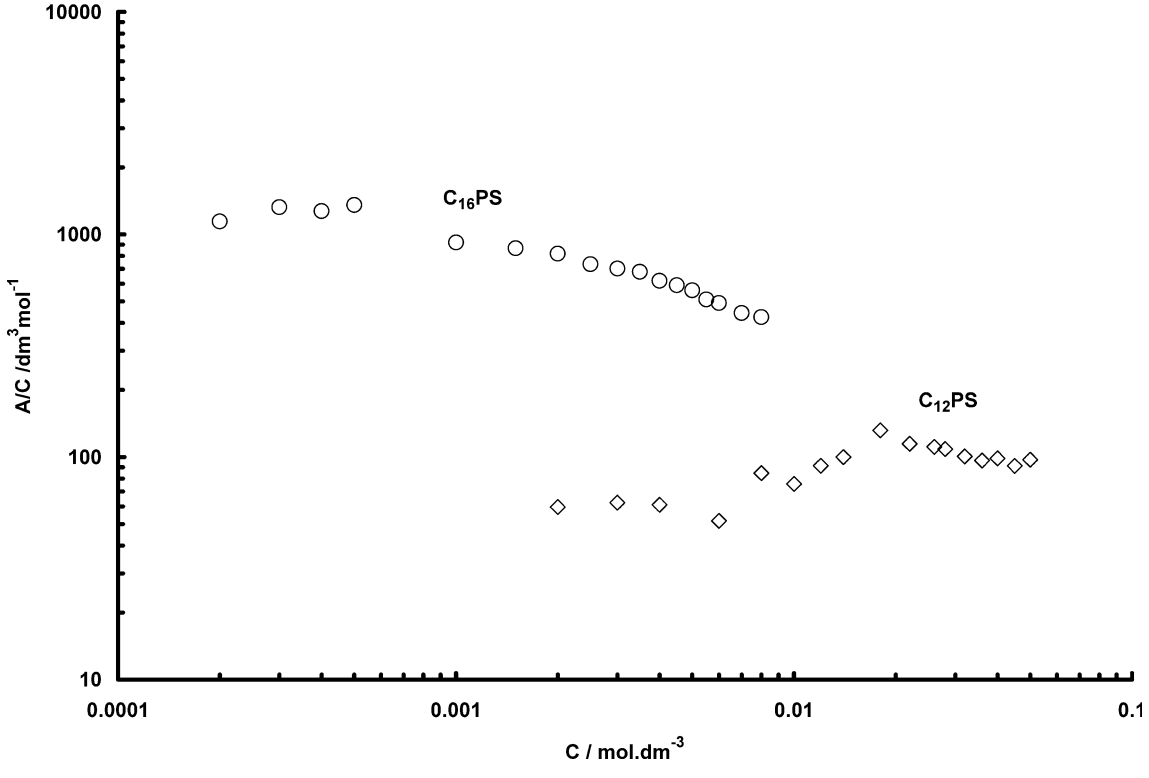

Fig. 7 Absorbance of solubilized Sudan III to surfactant concentration ratio for $C_{12}PS$ (*open diamonds*) and $C_{16}PS$ (*open circles*) aqueous solutions vs surfactant concentration

like transition. Furthermore, the micelle Stern layer has a polarity which is substantially different to that of pure water. Then the introduction of a polar head-group in the micelle Stern layer produces a change in the polarity of the microenvironment that also affects the absorptivity of chromophore groups. The expected effect is just that observed in Fig. 6. In particular, the more crowding, the larger deformation of the ring and the lower the absorptivity, because the conformation becomes less favorable to the delocalization, This is also seen in Fig. 6.

Accordingly is the interpretation of the differential conductivity plots by Sugihara et al. [50], that the conductivity of spherical micelles was $\Lambda^{d}_{sph.mic} = 86.5$ S.cm^2 eq^{-1}, and that for the rod-like micelles at the sphere-to-cylinder transition $\Lambda^{d}_{rodlike\ mic..} = 26.4$ S.cm^2 eq^{-1}. The strong reduction in Λ^{d} is caused by a reduction in micelle ionization and the increase in size and asymmetry of micelles.

The micelle ionization degree α is obtained from Evans' equation [51]:

$$1000(d\kappa/dC)_2 = n^{2/3}\alpha^2\left[1000(d\kappa/dC)_1 - \lambda_X\right] + \alpha\lambda_X \quad (1)$$

where $(d\kappa/dC)_1$ and $(d\kappa/dC)_2$ are the slopes of the κ vs C straight lines prior to and after the CMC, and λ_X is the equivalent conductivity of the counterion. We used $\lambda_{Br^-} = 77.4$ S cm^2 mol^{-1} [52]. Equation (1) is a quadratic function of α, because $(n-m) = n\alpha$. It is also dependent on n. However, this dependence is not strong and any reasonable value of n gives a good estimation of α [51]. The size of unmicellized $C_{12}PS$ is $n_{C12PS} = 11$ [24]. With $(d\kappa/dC)_1 = 0.086$ S dm^{3}cm^{-1} mol^{-1} and $(d\kappa/dC)_2 = 0.0277$ S dm^{3}cm^{-1} mol^{-1}, we obtained $\alpha_{C12PS} = 0.306$, in good agreement with the value found by McGrath and Drummond [25], and α_{C12PS} between 0.294 and 0.289 by using $n_{C12PS} = 51$. This value was obtained indirectly from surface tension measurements. By comparison, $\alpha = 0.195$ for dodecyltrimethylammonium bromide [53] and $\alpha = 0.31$–0.49 for sodium soaps [54].

The area per molecule (a) of the pure surfactant was computed from the surface tension plots of pure NaOL and pure NaDHC solutions, using the Gibbs' equation:

$$\Gamma_i = -\frac{1}{2RT}\frac{\partial\sigma}{\partial \ln C_i} \quad (2)$$

and the relationship $a_i = (\Gamma_i N_A)^{-1}$.

For $\Gamma = 1.17\times10^{-10}$ mol cm^{-2} and $a = 1.41$ nm^2 at the CMC, $\Gamma = 2.81\times10^{-10}$ mol cm^{-2}and $a = 0.592$ nm^{2}at the sphere-to-worm-like transition. McGrath and Drummond [25] found $a = 0.58 \pm 0.01$ nm^2 at 5.66×10^{-3} mol dm^{-3}, which is the CMC for these authors. This value is in agreement with that found by us at C_3. The a value is substantially higher than that of the transversal section of a saturated hydrocarbon chain (0.205 nm^2) [55] or 0.18 nm^2[56]. Values of $a_{molec} \geq 0.40$ nm^{2}are commonly found in soluble surfactant monolayers [57, 58]. This is associated with a disordered chain layer and water penetration between surfactant molecules [35]. The annular conformation proposed by Hamid and Shearringon [26] may also explain the high area per molecule at the air-solution interface, together with the electrostatic repulsion among these groups caused by the low ionic strength of the solution. However, the allyldimethyldodecylammonium bromide also shows a high a value at the CMC ($a = 0.58 \pm 0.01$ nm^2)[40], but it cannot form an annular structure.

$C_{16}PS$

The $\Delta\kappa$ vs C dependence for $C_{16}PS$ (not shown) also shows a curvature between $C = 1.39\times10^{-4}$ mol dm^{-3} and $C = 4\times10^{-4}$ mol dm^{-3} indicating that the aggregate structure (i.e., size and shape) gradually varies with concentration.

The differential conductivity for $C_{16}PS$ is shown in Fig. 1. Three steps may be seen two of them followed by regions of large slope that indicate gradual changes in size and shape dependent on concentration.

Table 2 shows the concentrations at which transitions were found in the diverse properties studied. These transitions occurred at $C_1 = (4.2 \pm 4.4)\times10^{-5}$ mol dm^{-3}, $C_2 = (1.42 \pm 0.24)\times10^{-4}$ mol dm^{-3}, $C_3 = (3.83 \pm 0.56)\times10^{-4}$ mol dm^{-3}, and $C_4 = (5.0 \pm 0.5)\times10^{-3}$ mol dm^{-3}.

The analysis of the diverse figures corresponding to this surfactant leads to the same conclusions to those in

Table 2 Transitions observed in $C_{16}PS$ solutions, in mol·dm^{-3}

Method	C_3	C_3	C_3	C_3
Λ(log C)	2.16×10^{-5}	0.000128	0.000253	-
$\Lambda(\sqrt{C})$	6.45×10^{-5}	0.000128	0.000416	-
$1000d\kappa/dC(C_{av})$	-	0.000133	0.00035	0.0052
$\Delta\kappa$(C)	-	0.000139	0.000426	-
κ(C)	-	0.000181	0.000416	-
σ(log C)	-	-	0.000565	-
δ(C)	-	0.0003	0.0045	-
η(C)	-	-	0.000323	0.00536
A(C)	-	-	0.000529	0.005
Sudan III	4.08×10^{-5}	-	0.0003	-
Average value	$(4.2 \pm 4.4)\times10^{-5}$	$(1.42 \pm 0.24)\times10^{-4}$	$(3.83 \pm 0.56)\times10^{-4}$	$(5.0 \pm 0.5)\times10^{-3}$

$C_{12}PS$ solutions. C_1 may be identified as the concentration in which pre-micelles start to form, C_2 may be interpreted as the CMC, and C_3 is associated with the transition spherical-to-cylindrical micelles. The fourth concentration (C_4) is probably associated with a new structural change. The viscosity increases the slope at C_4, which may be associated with an entanglement of the worm-like micelles. This entanglement occurs when the length of these micelles exceeds 100–125 nm [59]. The changes in the absorbance vs concentration curve (Fig. 6) may indicate some aggregates structural change affecting the molecular absorptivity of the surfactant. This may be associated with an increase in the crowding of the polar head-groups at the Stern layer, which alters the relative position of the diverse components of the ring.

The differential conductivity curve (Fig. 1) indicates that the aggregates occurring between C_2 and C_3, and between C_3 and C_4 change in shape and size with a strong dependence on concentration.

Tuin et al. [1] reported the $C_{16}PS$ CMC $= 4.89\times10^{-4}$ mol dm^{-3}, and Hamid and Sherrington [26] reported the CMC $= 5.84\times10^{-4}$ mol dm^{-3}. These values seem to indicate a confusion between the CMC and C_3. To compare, for hexadecylpyridinium bromide at 25 °C, CMC $= 6.0\times10^{-4}$ mol dm^{-3} [60], and for hexadecyltrimethylammonium methacrylate, CMC $= 9.8\times10^{-4}$ mol dm^{-3} [61]. The explanation for the differences is the same as in the $C_{12}PS$ case (see above).

According to the Sugihara et al. interpretation of differential conductivity [50], the $C_{16}PS$ spherical micelles have $\Lambda^{d}_{sph.mic.} = 89.5$ S cm^2 eq^{-1}, and the worm-like micelles at C_3, $\Lambda^{d}_{cyl.mic.} = 36.3$ S cm^2 eq^{-1}.

By application of Evans' equation with $n = 78.6$ [1], $(d\kappa/dC)_1 = 0.0972$ S dm^{3}cm^{-1} mol^{-1} and $(d\kappa/dC)_2 = 0.0794$ S dm^{3}cm^{-1} mol^{-1}, gave $\alpha_{C16PS} = 0.373$ at the CMC. From the literature, $\alpha_{C16PS} = 0.486$ [1]. To compare, for hexadecylpyridinium bromide at 25 °C, $\alpha = 0.43$ [60]. The higher value of α_{C16PS} when compared to α_{C12PS} is due to the lower CMC of the former, and in consequence, to the lower ionic strength in which $C_{16}PS$ micelles than those of $C_{12}PS$ are formed.

For $C_{16}PS$ at C_3 we found $\Gamma = 2.13\times10^{-10}$ mol cm^{-2}and $a = 0.778$ nm^2. In this case the sphere-to-cylinder transition did not produce the saturation of the air/solution interface. The cause may be the inter head groups repulsion because of the low ionic strength at C_3.

Conclusions

$C_{12}PS$ shows a three-step aggregation at the following concentrations:

- $C_1 = (7.78 \pm 0.27)\times10^{-4}$ mol dm^{-3}, at which pre-micellar aggregates form.
- $C_2 = (2.02 \pm 0.53)\times10^{-3}$ mol dm^{-3}, which is the CMC with spherical micelles, having an ionization degree $\alpha_{C12PS} = 0.306$ and micellar conductivity $\Lambda^{d}_{sph.mic} = 86.5$ S cm^2 eq^{-1}. The area per adsorbed molecule at the air/solution interface is $a = 1.41$ nm^2. There is an energetic advantage of the adsorbed monolayer over the micelles, giving rise to an increase in adsorption above the CMC.
- $C_3 = (6.94 \pm 0.36)\times10^{-3}$ mol dm^{-3}, that reflects the sphere-to-cylinder micelle transformation with $\Lambda^{d}_{mic.cil.} = 26.4$ S cm^2 eq^{-1} and $a = 0.592$ nm^2. Micelles become more energetically favored than the adsorbed monolayer.

$C_{16}PS$ shows a four-step aggregation at the following concentrations:

- $C_1 = (4.2 \pm 4.4)\times10^{-5}$ mol dm^{-3}, at which per-micellar aggregates form.
- $C_2 = (1.42 \pm 0.24)\times10^{-4}$ mol dm^{-3}, which is the CMC with spherical micelles, having an ionization degree $\alpha_{C12PS} = 0.373$ and micellar conductivity $\Lambda^{d}_{sph.mic} = 89.5$ S cm^{2}eq^{-1}.
- $C_3 = (3.83 \pm 0.56)\times10^{-4}$ mol dm^{-3}, that reflects the sphere-to-cylinder micelle transformation with $\Lambda^{d}_{mic.cil.} = 36.3$ S cm^2 eq^{-1} and $a = 0.778$ nm^2. Micelles become more energetically favored than the adsorbed monolayer.
- $C_4 = (5.0 \pm 0.5)\times10^{-3}$ mol dm^{-3}, which probably corresponds to an entanglement of the worm-like micelles.

In both surfactants, the additional reduction of the CMC over that corresponding to the increase in hydrophobicity caused by the additional methylene groups may be explained by the reduction in polarity because of the charge delocalization caused by the annular conformation of the head group. This delocalization causes a reduction in the polar head group hydrophilicity. The ring deformation caused by the crowding of the polar head groups at the micelle Stern layer (and possibly the change in the microenvironment polarity when these groups are included in the micelle electrical double layer coming from water) may cause the changes in adsorptivity at the CMC and when the structure of micelles change.

Acknowledgement This work was supported by the project # 38681-E from CONACYT of Mexico

References

1. Tuin G, Candau F, Zana R (1998) Colloids Surf A 131:303
2. Laschewsky A (1995) Adv Polym Sci 124:1
3. Renoux D, Selb J, Candau F (1994) Progr Colloid Polym Sci 97:213
4. Volpert E, Selb J, Candau F (1996) Macromol 29:1452
5. Chang Y, McCormick CL (1993) Macromol 26:6121
6. Paleos CM, Hristiades C, Evangelatos GP, Dias P (1982) J Polym Sci Polym Chem Ed 20:2565
7. Nagai N, Ottishi Y, Inaba H, Kudo SJ (1985) J Polym Sci Polym Chem Ed 23:1221
8. Kunitake T, Nagai M, Yanangi H, Takarabe K, Nakashima N (1984) J Macromol Sci Chem A21:1237
9. Kusumi A, Singh M, Tirrell DA, Oehme G, Singh A, Samuel NKP, Hyde JS, Regen SL (1983) J Am Chem Soc 105:297
10. Chung Y-C (1997) Bull Korean Chem Soc 18:1041
11. Laschewsky A, Ringsdorf H, Schmidt G, Schneider J (1987) J Am Chem Soc 109:788
12. Goettgens BM, Tillmann RW, Radmacher M, Gaug HE (1992) Langmuir 8:1768
13. Suh J, Shin S, Shim H (1997) Bull Korean Chem Soc 18:190
14. Kunitake T, Nakashima N, Kunitake M (1989) Macromol 22:3544
15. Thundathil R, Stoffer JO, Friberg SE (1980) J Polym Sci Chem Ed 18:2629
16. Sisson T, Srisiri W, O'Brien DF (1998) J Am Chem Soc 120:2322
17. Full AP, Puig JE, Gron LU, Kaler EW, Minter JR, Mourey TH, Texter J (1992) Macromol 25:5157
18. Puig JE, Corona-Galván S, Maldonado A, Schulz PC, Rodríguez BE, Kaler EW (1990) J Colloid Interface Sci 137:308
19. Li TD, Gan LM, Chew CH, Teo WK, Gan LH (1996) Langmuir 12:5863
20. Soltero JFA, Gonzalez Alvarez A, Puig JE, Manero O, Schulz PC, Rodriguez JL (1998) Colloids Surf A 145:121
21. McGrath KM (1996) Colloid Polym Sci 274:499
22. Shibasaki Y, Fukuda K (1992) Colloids Surf 67:195
23. Uang Y-J, Blun FD, Friberg SE, Wang J-F (1992) Langmuir 8:1487
24. Nika G, Paleos CM, Dais P (1992) Progr Colloid Polym Sci 89:122
25. McGrath KM, Drummond CJ (1996) Colloid Polym Sci 274:612
26. Hamid S, Sherrington D (1987) Polymer 28:325
27. McBain JW, Baker L (1935) Trans Faraday Soc 31:149
28. Kolthoff J, Stikews K (1948) J Phys Chem 52:916
29. Jones MN, Bury CR (1927) Phil Mag 4:841
30. Schulz PC, Lelong ALM (1979) Anales Asoc Quím Argentina 67:41
31. Miguens N (1977) PhD Thesis, Universidad Nacional del Sur, Bahía Blanca, Argentina
32. Schulz PC (1988/89) Colloids Surf 34:69
33. Schulz PC (1989) Afinidad XLVI 423:433
34. Schulz PC (1995) Colloid Polym Sci 273/3:288
35. Lu JR, Simister EA, Lee EM, Thomas RK, Rennie AR, Penfold J (1992) Langmuir 8:1837
36. Lu JR, Lee EM, Thomas RK, Penfold J, Flitsch SL (1993) Langmuir 9:1352
37. Lu JR, Li ZX, Thomas RK, Penfold J (1996) J Chem Soc Faraday Trans 92:403
38. Lu JR, Marrocco A, Su TJ, Thomas RK, Penfold J (1993) J Colloid Interface Sci 158:303
39. Paleos C, Dais P, Mallinaris A (1984) J Polym Sci Part A Polym Chem Ed 22:3383
40. McGrath KM, Drummond CJ (1996) Colloid Polym Sci 274:316
41. Tartar HV, Lelong ALM (1955) J Phys Chem 59:1185
42. Chevalier Y, Soret Y, Poorchet S, Le Perchec P (1991) Langmuir 7:848
43. Ralston AW, Eggenberger DN, Harwood H (1947) J Am Chem Soc 69:2095
44. Mysels KJ (1959) J Colloid Sci 10:507
45. Mast RC, Haynes LV (1975) J Colloid Interface Sci 53:35
46. Khalil OS, Sonnessa A (1977) J Mol Photochem 8:399
47. Minardi RM, Schulz PC, Vuano B (1997) Colloid Polym Sci 275:754
48. Schulz PC (1991) Colloid Polym Sci 269:612 and references cited therein
49. Schulz PC (1991) J. Colloid Interface Sci 152:333 and references cited therein
50. Sugihara G, Era Y, Funatsu M, Kunitake T, Lee S, Sasaki Y (1987) J Colloid Interface Sci 187:435
51. Evans HC (1956) J Chem Soc Part 1:579
52. (1975/1976) Handbook of chemistry and physics, 56th edn. CRS Press, Cleveland
53. Ingram T, Jones MN (1969) Trans Faraday Soc 65(1):297
54. Ekwall P, Stenius P (1967) Acta Chem Scand 21:1767
55. McBain JW, Bolduan OEA, Ross S (1941) J Am Chem Soc 65:1873
56. Clint JH (1992) Surfactant aggregation. Blackie, Glasgow, p 95
57. Denton AR, Gray CG, Sullivan DE (1994) Chem Phys Lett 219:310
58. Rosen MJ (1976) J Colloid Interface Sci 56:320
59. Schulz PC, Zapata-Ormachea ML (1994) Colloid Polym Sci 272:1259
60. Vojteková M, Kopecky F, Greksáková O (1994) Collect Czech Chem Commun 59:99
61. Lerebours B, Perly B, Pileni MP (1988) Chem Phys Lett 147:503